

Review

New Trends in Uric Acid Electroanalysis

Ligia Chelmea^{1,2,3}, Mihaela Badea^{1,2,*} , Ioan Scarneciu⁴, Marius Alexandru Moga⁴, Lorena Dima^{1,2} , Patrizia Restani⁵ , Cecilia Murdaca⁵, Daniel Ciurescu⁴ and Laura Elena Gaman⁶

- ¹ Department of Fundamental, Prophylactic and Clinical Disciplines, Faculty of Medicine, Transilvania University of Brasov, 500019 Brasov, Romania; ligia.chelmea@unitbv.ro (L.C.); lorena.dima@unitbv.ro (L.D.)
- ² Research Center for Fundamental Research and Prevention Strategies in Medicine, Research and Development Institute of the Transilvania University of Brasov, 500484 Brasov, Romania
- ³ Department of Infectious Diseases, Pulmonology and Infectious Diseases Clinical Hospital of Brasov, 500174 Brasov, Romania
- ⁴ Department of Medical and Surgical Specialties, Faculty of Medicine, Transilvania University of Brasov, 500019 Brasov, Romania; ioan.scarneciu@unitbv.ro (I.S.); mogas@unitbv.ro (M.A.M.); daniel.ciurescu@unitbv.ro (D.C.)
- ⁵ Faculty of Pharmacy, Università degli Studi di Milano, 20133 Milan, Italy; patrizia.restani@unimi.it (P.R.); c.murdaca@hotmail.it (C.M.)
- ⁶ Faculty of Medicine, Carol Davila University of Medicine and Pharmacy, 020021 Bucharest, Romania; laura.gaman@umfcd.ro
- * Correspondence: mihaela.badea@unitbv.ro

Abstract: Considering the increasing incidence of hyperuricemia and oxidative stress-related diseases, quantification of uric acid has become essential. Therefore, the evolution on sensing devices being favorable, these questions are more often addressed to the field of medical researchers. As for many metabolites, (bio)sensors provide a reliable method for screening and evaluation of uric acid status. Due to the numerous categories of (bio)sensors available, choosing the appropriate one is a challenge. This study reviews the scientific information concerning the most suitable (bio)sensors for quantification of uric acid, presenting a list of sensors from the last decade, categorized by configurations and materials. In addition, this review includes a comparison of sensors according to their interference behavior and sensitivity, offering an objective perspective for identifying devices that are suitable for clinical applications.

Keywords: uric acid; chemosensors; biosensors; nanocomposites; electroanalysis; urine; clinical applications



Citation: Chelmea, L.; Badea, M.; Scarneciu, I.; Moga, M.A.; Dima, L.; Restani, P.; Murdaca, C.; Ciurescu, D.; Gaman, L.E. New Trends in Uric Acid Electroanalysis. *Chemosensors* **2023**, *11*, 341. <https://doi.org/10.3390/chemosensors11060341>

Academic Editor: Daniele Merli

Received: 1 May 2023

Revised: 1 June 2023

Accepted: 6 June 2023

Published: 9 June 2023



Copyright: © 2023 by the authors. Licensee MDPI, Basel, Switzerland. This article is an open access article distributed under the terms and conditions of the Creative Commons Attribution (CC BY) license (<https://creativecommons.org/licenses/by/4.0/>).

1. Introduction

Uric acid is a metabolic product that results from degradation of purines in the liver. Usually, uric acid is identified from biological fluids, human serum and urine through conventional methods, such as spectroscopy, chromatography, electrochemistry, membrane capillary electrophoresis and spectrophotometric methods, including uricase enzymatic reactions [1]. Importantly, uric acid determination opens the possibility of early intervention in cases of hyperuricemia and preventing the degradation of renal function.

From the electrochemical point of view, uric acid is a weak acid, with two-step dissociation at a pK_{a1} of 5.4 and a pK_{a2} of 9.8. In the physiological range of pH (7.35–7.45), in the extracellular compartment, uric acid is found mostly (98%) in the form of biurate (deprotonated urate anion or ionized urate), and a very small quantity (<1%) is found as undissociated uric acid [2]. However, in more acid pH media, such as urine (pH 6.5), uric acid is still found mainly as biurate (88%) but with an increased percentage as uric acid (12%) [2,3].

The physiological levels of uric acid are between 3.5 mg/dL and 7.2 mg/dL (210 μ M and 430 μ M) in males, and between 2.6 mg/dL and 6.0 mg/dL (155 μ M and 360 μ M) in

premenopausal females [2]. These levels are maintained by exogenous input (diet) but mostly by endogenous formation (nucleic acid catabolism and de novo synthesis) [4].

At high levels of uric acid, hyperuricemia, the undissociated uric acid precipitates at the vascular level and biurate is implicated in kidney stones formation. This phenomenon occurs because of the low solubility (6 mg/dL or 360 μ M) of uric acid, mainly in the form of monosodium urate [2].

The oxidation of uric acid starts with the formation of diimine (a) by exchanging $2e^-$ and $2H^+$. The resulting diimine takes up two molecules of water and forms imine-alcohol (b) and uric acid-4,5-diol (c), successively. Ultimately, uric acid-4,5-diol is decomposed to allantoin (d) and CO_2 in neutral pH (Figure 1) [5].

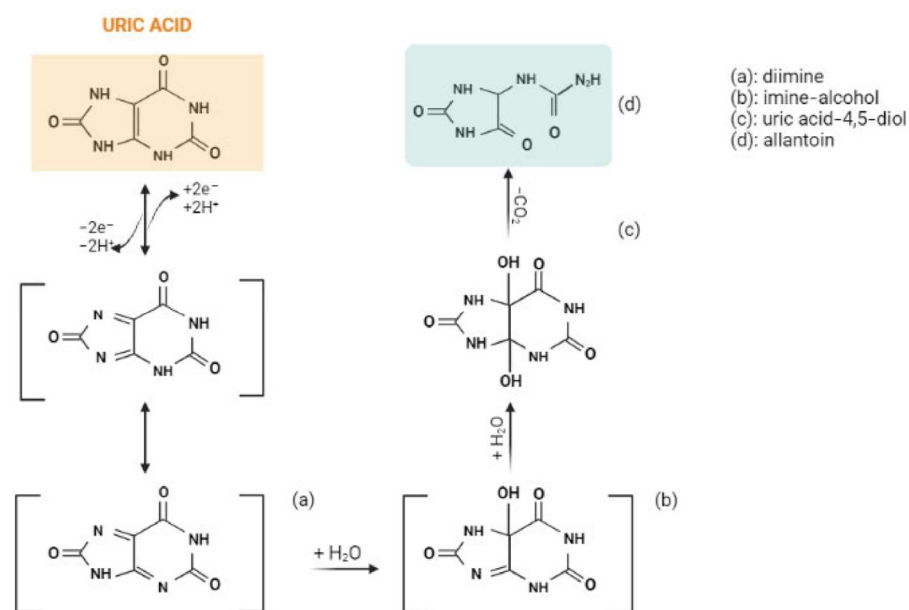


Figure 1. The electrochemical oxidation of uric acid to allantoin. Created with BioRender.com.

The oxidative properties of uric acid can be used in developing catalytic methods of detection. Thanks to the high electrochemical capacity of uric acid, for the rapid quantification of uric acid levels, scientists have developed different uric acid detection tools.

Together with uric acid, dopamine and ascorbic acid have similar oxidative behavior and coexist in urine samples [6]. Therefore, uric acid, dopamine and ascorbic acid signals can interfere with each other in the process of electrochemical detection in real samples. These three compounds have a very similar oxidation potential, so their electrochemical detection is very challenging [6] as obtaining separate voltametric peaks is the principal objective [7]. This matter has been investigated frequently for most types of electrodes, such as conventional sensors, modifiable electrodes and biosensors.

However, dopamine, uric acid and ascorbic acid have individual and cumulative importance because of their role in oxidative stress-related diseases [8]. Parkinson's disease, most of all, lacks a rapid diagnostic method using biological markers for diagnosis of the early stages of the pathology [9] and it is an example where simultaneous detection of the three compounds may be useful [10].

Other cases in which it may be important to establish levels of uric acid and its electrochemically similar compounds, dopamine and ascorbic acid, in biological matrixes are the following: dopamine: cardiotoxicity [11], aging [12], multiple sclerosis [13], rheumatoid arthritis [13], Alzheimer's disease [13], and Tourette [13]; uric acid: arthritis [14], gout [14], Lesch–Nyhan syndrome [14], urolithiasis [14], kidney damage [14], leukemia [15], lymphoma [15], and multiple sclerosis [16]; and ascorbic acid: high blood pressure [17], heart attack risk [17], cataracts [17], tooth decay [17], improper bone development [17], loss

of appetite [17], weakened cartilage [17], skin hemorrhages [17], impaired digestion [17], septic shock [18], and diabetes mellitus [19].

The aim of this paper is to outline the variety of electrodes developed in the last ten years for quantification of uric acid. We investigate different types of modified electrodes and biosensors, comparing their sensitivity, specificity and efficiency for applications in the medical field.

2. Methodology

We include pertinent studies written in English that were published between 2012 and 2022 and also several older publications. The studies were identified in the PubMed database using relevant keywords including “uric acid detection”, “uric acid electroanalysis”, “uric acid electrochemical sensors”, “uric acid biosensors”, and “electrochemical urine test”. Considering the purpose of this review, relevant data were also selected based on their medical application.

3. Results and Discussion

An abundance of sensors has been developed to detect uric acid from standard solutions and real samples, so this review outlines a wide variety of electrodes based on the type and configuration of materials and the electrodes' behavior in relation to interferent compounds (Figure 2).

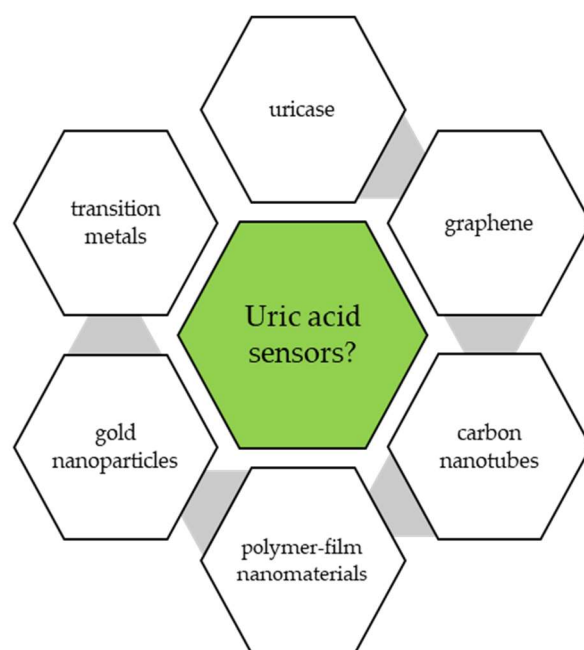


Figure 2. Types of modification elements in uric acid electrochemical sensors.

Results show a good linearity for increasing analyte concentration and a low limit of detection (LOD) for most sensors and biosensors. However, it has to be considered that some require expensive materials, such as platinum [7] or gold [20], or surface modifications and activation reactions. Others utilize electrochemical copolymerization [21], functionalization with nanoparticles [22], or electro activation with enzymes [23], which usually require more time and resources as their functionalization needs to be verified and controlled before use [24].

In the past ten years, a large variety of electrochemical sensors for detection of uric acid and interferent compounds (ascorbic acid, dopamine) have been characterized [25]. Based on the studies reviewed, there appears to be a large group of highly sensitive sensors for detection and quantification of uric acid from serum or urine samples [25].

Non-enzymatic sensors are the most common electroanalysis device for detection of urinary compounds, but biosensors are a feasible alternative [26]. Some common modifications of sensors include using glassy carbon electrodes, graphene oxide electrodes or carbon nanotubes [26].

Carbon electrodes provide a large potential window [27,28], good conductivity [28,29] and are electrochemically inert [29], which offers stability and versatility for detection techniques. Graphene oxide (GO) [27,28,30–35] and other composites [27,29,32,34,35] can be used for improving the glassy carbon electrode through surface modifications. Graphene oxide has useful electrochemical properties [29], such as hydrophilicity [36], and facile biomolecule adsorption and electron transfer [26,37]. Moreover, graphene hybrids and their bio-derivates offer great biocompatibility and improved chemical interaction with viable cells, but with some limitations [38].

Broadly, there are several major types of modification path-transition metal-modified electrodes (Table 1), including gold-coated electrodes (Table 2), chemically modified electrodes (Table 3) and biosensors (Table 4). In addition, this article presents an overview of the main types of newly developed electrodes.

3.1. Sensors for Uric Acid Electroanalysis

3.1.1. Transition Metal Nanoparticles for Uric Acid Detection

It has been demonstrated that transition metal oxide nanoparticles can be used widely in electrochemical detection due to their high biocompatibility, electrochemical stability and good conductivity [39–41]. In addition, their low cost and wide availability are advantageous characteristics, especially regarding titanium and palladium [39,42].

Their photocatalytic and electrochemical properties are based on high their hydrophobicity, electron-rich state, good conductivity and biocompatibility. The conductivity of these materials results from hybridization of the d orbital of the metal ion and the p orbital of the oxygen atoms [43]. Their shape, size and large surface area offer improved stability and sensitivity due to electron transfer process and the adsorption of the biomolecules [39,43].

In particular, CuO enables better selectivity and sensitivity due to its narrow band gap energy of 1.2 eV to 1.5 eV and anode electrochemical charging. Additionally, CuO has high catalytic activity, a nontoxic nature, high optical absorption and is low cost, making it suitable for electrochemical applications [40].

This review covers some recently developed electrodes (Table 1) and expands on several examples of different electrode configurations.

- Glassy carbon electrode coated with titanium dioxide nanoparticles.

Titanium dioxide (TiO₂) has wide applicability in the configuration of electrochemical sensors and biosensors, in water treatment and in other domains [39,44–47]. This transition metal oxide is harmless and highly chemically stable [40].

Rajeswari et al., present a new titanium nanoparticle-coated glassy carbon electrode for detection of uric acid (UA), which was tested in standard solutions and real urine samples [39]. The sensor was morphologically characterized by scanning electron microscopy (SEM) and energy dispersive X-ray analysis (EDX) techniques. Under optimized conditions, the electrochemical measurements were performed by differential pulse voltammetry (DPV) in a neutral medium (phosphate buffer solution, pH 7.0). The oxidation peaks of uric acid appeared in a concentration range of 1 μM to 9 μM, with a limit of detection at 0.764 μM. Regarding the real urine samples tests, a TiO₂NPs/GCE sensor demonstrated high selectivity against urine interferent compounds, with a recovery of 97.0% to 99.6%, which makes it suitable for medical applications [39].

- Palladium nanoparticles/reduced graphite oxide nanocomposites.

Palladium nanoparticles are another type of advantageous transition metal nanoparticles. They are similar to titanium [39] because of their rapid electron transfer, high conductivity, low cost and good electrochemical stability [39,42,48]. A novel nanocomposite, consisting of palladium nanoparticles (PdNPs) and reduced graphene oxide was

demonstrated to detect uric acid, dopamine and ascorbic acid. After the construction of the sensor, CV and EIS measurements were successfully performed. Under optimal conditions, the best peak potential for UA, DA and AA was determined using the DPV technique in a phosphate buffer solution of pH 7.2. The detection limit was comparable with other electrodes measurements (Table 2) at 0.1 mM, 1 μ M, and 16.67 μ M for AA, DA and UA, respectively. Additionally, the detection linear ranges were low at 0.5 mM to 3.5 mM (AA), 3 μ M to 15 μ M, 15 μ M to 42 μ M (DA), and 0.3 μ M to 1.4 mM (UA) [43]. The electrode showed good separation of peaks, discriminating between analytes present in human serum samples, with recovery rates from 96.6% to 108.5% [43].

- A glassy carbon electrode coated with copper oxide.

Copper oxide nanoparticles, as well as NiO, SnO, ZnO, CO₃O₄, and MgO, are suitable for use in electrochemical devices, such as sensors and biosensors [40,48,49]. One configuration of a copper nanoparticle-based electrode is the CuO/GCE electrode for detection of uric acid (UA). The electrode was morphologically characterized by XRD, FESEM and EDS. Uric acid was subjected optimally to cyclic voltammetry measurements in a phosphate buffer of pH 7.4. According to the optimization parameters, the best anodic peak potential of uric acid was found at 0.4 mV, with a limit of detection of 0.6 μ M and at linear range of 0.001 mM to 351 mM. The selectivity of the electrode was successfully demonstrated in urine samples tests, with recovery rates from 95.56% to 104% [40].

Table 1. Comparison of electrodes modified with transition metal nanoparticles for detection of uric acid.

Electrode	Technique	pH	Interference	Biological Sample; Relative Recovery (RR)	UA Linear Range (μ M)	UA LOD (μ M)	Ref.
GCE/MC-GO-Fe ₃ O ₄ ¹	CV, DPV	7.0	UA, AA, DA, G, sucrose, L-Cys, citric acid, Fe ²⁺ , Cl ⁻ , Na ⁺ , NO ₃ ⁻	Human urine RR > 96%	0.5–140	0.17	[37]
TiO ₂ NPs/GCE ²	DPV	7.0	UA	Human urine RR: 97–99.6%	1–9	0.764	[39]
PdNPs/rGO/GCE ³	DPV	7.2	UA, AA, DA	Human serum RR: 96.6–108.5%	0.3–1400	16.67	[42]
SnO ₂ /chitosan/GCE ⁴	DPV		UA, AA, DA	Human urine RR: 97.4%	3–200	1	[50]
CuO/GCE ⁵	CV	7.4	UA, UR, lactic acid, ethanol, G, K ⁺ , Na ⁺	Human urine RR: 95–104%	0.001–351,000	0.6	[40]
RuON-GCE ⁶	DPV	7.0	UA, E	Human urine RR: 98–101.6%	3.0–56.6; 56.6–758.6	0.47	[51]
MoS ₂ NSA/CNFs ⁷	CV, DPV	7.0	UA, levodopa	Human urine RR: 99.7–102.6%	1–60	1	[52]
CuO nano-rice/GCE ⁸	CV, DPV	7.0	UA, AA, DA, G, fructose, galactose, lactose, Na ⁺ , Cl ⁻ , K ⁺ , Ca ²⁺ , Br ⁻ , CO ₂ ³⁻ , NH ₄ ⁺ , NO ₂ ⁻ , NO ₃ ⁻ , SO ₄ ²⁻ , SO ₃ ²⁻	Human urine RR: 98.6–102.6%	1–60	1.2	[53]
Fe ₃ O ₄ @CNT-N/GCE ⁹	SWV	2.5	UA, AA, DA	-	25–85	0.47	[22]
ZnO NWAs/GF/GCE ¹⁰	DPV	7.4	UA, AA, DA	Human serum	0–40	0.001	[24]

AA = ascorbic acid, Cys = cysteine, DA = dopamine, E = epinephrine, G = glucose, SWV = square wave voltammetry, UA = uric acid, UR = urea; ¹ = Glassy carbon electrode based on modified methylcellulose by graphene oxide and Fe₃O₄ nanoparticles; ² = Glassy carbon electrode coated with titanium dioxide nanoparticles; ³ = Palladium nanoparticles/reduced graphite oxide nanocomposite on a glassy carbon electrode; ⁴ = SnO₂ nanoparticles/multi-walled carbon nanotubes/carbon paste electrode; ⁵ = Glassy carbon electrode coated with copper oxide; ⁶ = Glassy carbon electrode modified with ruthenium oxide nanoparticles; ⁷ = MoS₂ nanosheet arrays/carbon nanofibers; ⁸ = CuO nano-rice-modified glassy carbon electrode; ⁹ = N-doped carbon nanotubes functionalized with Fe₃O₄ nanoparticles; ¹⁰ = Glassy carbon electrode modified with ZnO nanowire arrays on 3D graphene foam.

3.1.2. Gold-Coated Electrodes

Gold nanoparticles have demonstrated good stability and biocompatibility [54]. Gold is the most stable transition metal in electrochemical analysis [55], but its main drawback is the cost. Despite this, recently, a series of gold nanoparticle composite electrodes have been manufactured and tested successfully for detection of uric acid and interferent compounds (Table 2) [27,29–36]. Because of the high conductivity properties of gold nanoparticle [27,56], this metal is preferred for the configuration of sensors [27]. In addition to gold nanoparticles, the most used component for the sensor base are glassy carbon electrodes (GCE) [28]. In combination with reduced graphene oxide (rGO), the sensitivity of the sensor can be increased by reducing the detection limit and amplifying the electric signal [57]. This effect results from graphene's properties as a two-dimensional carbon material with a large surface area and high conductivity. One important drawback of graphene is the hydrophobic properties resulting from the π - π interactions between individual layers, which reduce the solubility [58].

Thus, in the oxidized form, GO provides hydrophilicity and increased catalytic properties through the presence of negatively charged groups of oxygenated functional groups (hydroxyl, carboxyl and epoxy groups), although GO is less conductive than the non-oxidized form. In order to achieve better conductivity, GO was combined with conductive materials, such as conductive polymers (polypyrrole, poly(3,4-ethylenedioxythiophene), polyaniline and others) [30].

Table 2 presents different types of highly sensitive gold-coated sensors for detection of uric acid and interferent compounds, as well as a short overview of some electrodes.

- Au nanorod-decorated graphene oxide (GO/AuNR) glassy carbon electrode (GCE).

This material designed by Safitri et al., consists of a modified glassy carbon electrode with a graphene oxide and gold nanorod covering and was designed and optimized for detection of uric acid [27]. The graphene oxide was synthesized by the modified Hummers' method [59], and the synthesis of the gold nanorods was performed using the Nikoobakht and El-Sayed method [27,59]. The design, statistical and mathematical analysis and optimization were performed with specialized software, and the influence of GO and AuNR on the uric acid oxidation curves was studied using a central composite design (CCD) method. The deposition of the two composites onto the electrode was characterized by TEM, SEM, EDS and XDR images. The measurements were performed with a three-electrode cell potentiostat-working electrode (glassy carbon electrode), a reference electrode (Ag/AgCl electrode) and an auxiliary electrode (platinum wire electrode) [27].

The optimization study was performed with the differential pulse voltammetry (DPV) technique and cyclic voltammetry (CV). However, the DPV technique demonstrated higher sensitivity and peak isolation in comparison with CV. For DPV, the optimum experimental parameters were established: the uric acid peak potential was between +0.2 V and +1.0 V, with a 50 mV s⁻¹ scan rate, a potential step of 5 mV, a potential pulse of 25 mV, and a pulse time of 0.01 s. The standard calibration curve represented the relation between the concentration of uric acid and the potential peak current of uric acid. The measurements were performed for a uric acid concentration range of 10 μ M to 90 μ M in KCl solution. The results showed a LOD at 0.4 μ M and a quantification limit of 1.0 μ M, which is comparable to other highly sensitive uric acid sensors [27,30,37,60–64]. The electrode exhibited good stability and selectivity, as shown in Table 2, by performing repeated measurements in the presence of ascorbic acid (AA), dopamine (DA), glucose (G), magnesium and urea (UR). Moreover, it was used to perform real urine sample tests with satisfactory results [27].

- Gold Nanoparticle-Decorated Polypyrrole/Graphene Oxide Nanosheets.

Tan et al., present an electrode based on carbon fiber paper, modified with a polypyrrole/graphene oxide composite and coated with gold nanoparticles [30]. It combines non-reduced GO with polypyrrole (PPy) for better conductivity. The electrode was evaluated using SEM and EDS images. The measurements performed using DPV in a neutral medium (pH 7.0) indicated a linear range between 2 μ M and 360 μ M for uric acid (UA),

with a detection limit at 1.68 μM . An investigation of the electrode's behavior in the presence of ascorbic acid (AA) and dopamine (DA) showed a high selectivity for uric acid. The linear ranges for AA and DA were 10 μM to 1600 μM and 0.2 μM to 60 μM ; the LOD values for AA and DA were 2.43 μM and 0.115 μM , respectively. Additionally, the same conditions were applied for analysis of real samples and provided good results. Among the electrodes presented in Table 2, the AuNPs@GO/PPy/CFP electrode showed good selectivity but still requires improvement in terms of LOD and detection range [30].

- ITO-rGO-AuNPs electrode for uric acid detection.

This new flexible electrode is based on a polyethylene terephthalate (PET) substrate coated with indium tin oxide (ITO) and combined with reduced graphene oxide (rGO) and gold nanoparticles (AuNPs) [65]. The characterization of the sensor was performed with EDS and SEM analyses. Uric acid detections were performed by linear sweep voltammetry (LSV) and appeared at 0.4 V. In the optimization study, uric acid showed the best oxidation potential at pH 8 in nitrate buffer solution, with a limit of detection of 3.6 μM and a linear range between 10 μM and 500 μM . The measurements were performed with a three-electrode cell (standard calomel electrode (reference), Pt wire (counter electrode), and ITO-rGO-AuNPs (working electrode)). The interference test was performed in the presence of a high concentration of ions (ammonium, chloride and sodium) and ascorbic acid, with an insignificant effect on the uric acid curve [65]. Finally, testing of real samples (milk and urine) showed results comparable with those of other devices and validated the sensor for medical applications [65].

- Poly(diallyldimethylammonium chloride)-functionalized reduced graphene oxide and polyoxometalates-doped Au nanoparticle sensor

Bai et al., configured a sensitive sensor by combining poly(diallyldimethylammonium chloride) (PDDA) with graphene sheets and polyoxometalates-doped Au nanoparticles [34]. This configuration is advantageous for the detection of uric acid because of the attraction between the positively charged polyelectrolytes and non-covalently functionalized graphene sheets [34,66,67]. In addition, the presence of gold nanoparticles enhances the electrode stability through electrostatic attraction. The configuration of the composite was investigated using atomic force microscopy (AFM), SEM and X-ray photoelectron spectra (XPS) [30].

Measurements were performed by a three-cell electrode consisting of the working electrode (composite film-modified electrode coated on ITO), a counter electrode (a twisted platinum wire) and a reference electrode (Ag/AgCl) in a phosphate buffer solution of pH 7.0. Uric acid was tested under optimized conditions and showed high sensitivity and good interference stability. The suitable analytical technique for this electrode was DPV, which revealed a uric acid peak at +350 mV, with a detection range between 2.5×10^{-7} and 1.5×10^{-4} and an LOD value of 0.08. In terms of stability, the sensor appeared to have long-term storage stability, even after 28 days of storage in dry conditions at room temperature. An interference study of the electrode was performed with human urine samples and demonstrated good average recovery of 97.92% [34].

- A sensor based on reduced graphene oxide functionalized by poly(amido-amine), multi-walled carbon nanotubes and Au nanoparticles.

Another type of sensor differing from other reduced graphene oxide-Au composites (Table 2) was created and characterized by Wang et al. [35]. For the configuration of this nanohybrid, RGO-PAMAM-MWCNTs-AuNPs, the authors utilized reduced graphite oxide as the sensor base in combination with poly(amido-amine) (PAMAM) dendrimers and multi-walled carbon nanotubes coated with gold nanoparticles for higher performance in the detection of uric acid and interferent molecules.

PAMAN dendrimers have a branched structure that benefits future synthesis and confers structural homogeneity, mostly in the presence of metal nanoparticles [35,68–71]. SEM images were used to study the sensor's morphology. The sensor optimization for detection of uric acid (UA), ascorbic acid (AA) and dopamine (DA) showed an optimal

pH of 4.0 in phosphate buffer solution when performing differential pulse voltammetry (DPV) [35].

Regarding the interference study, in the mixture of the three compounds, three separate anodic peaks were detected at 0.06 V, 0.32 V and 0.44 V, corresponding to AA, DA and UA, respectively. The electrochemical signal appeared in the linear ranges of 20 μM to 1.8 mM, 10 μM to 0.32 mM, and 1 μM to 0.114 mM for AA, DA and UA, respectively, with detection limits at 6.7 μM , 3.3 μM and 0.33 μM . Despite the fact that no real samples were tested, this sensor showed promising results with good catalytic activity and high sensitivity, providing a visible peak separation between the interferent compounds [35].

- Nafion-based electrode modified with Azure A-coated carbon nanotubes coated with gold nanoparticles.

A different multi-walled carbon nanotubes composite was created, but in contrast to RGO-PAMAM-MWCNTs-AuNPs [35], it was prepared on a nafion base with N0, N0-dimethylphenothiazin-5-ium-3,7-diamine (AzA) molecules attached to the multi-walled nanotubes and coated with gold nanoparticles [36]. The AzA molecules were chosen because of the strong interaction between their positive charge and the negative charge of the carboxyl groups of MWCNTs [36,66,67]. This bond provides stability to the composite in electrochemical detections [32,72,73]. The performance of the sensor was demonstrated by testing AA, DA, UA and tryptophan (Trp) in a phosphate buffer solution of pH 7.0 in a mixture of solutions and also from real urine and milk samples. For the characterization of the sensor morphology, TEM images were obtained [36].

The electrochemical detections were performed with a three-cell system, consisting of a working electrode (Nafion/AuNPs/AzA/MWCNTs), a counter electrode (Platinum wire) and a reference electrode (Ag/AgCl electrode). The differential pulse voltammetry (DPV) technique was chosen for detection of a mixture of four compounds (AA, DA, UA and Trp), with variation in the concentration of a single compound at each test. The results showed linear ranges for AA, DA, UA and Trp at 300 μM to 10,000 μM , 0.5 μM to 50 μM , 0.5 μM to 50 μM and 1.0 μM to 100 μM , respectively, and detection limits at 16 μM , 0.014 μM , 0.028 μM and 0.56 μM , respectively. The time stability of the sensor was demonstrated by a 93.7% response after 20 days of storage. Additionally, in measurements of real samples, the sensor displayed no interference with other compounds, which indicates very good selectivity of the sensor [36].

Table 2. Comparison of gold-coated electrodes for detection of uric acid.

Electrode	Technique	pH	Interference	Biological Sample. Relative Recovery (RR)	UA Linear Range (μM)	UA LOD (μM)	Ref.
GO/AuNR/GCE ¹	DPV	-	UA, AA, DA, G, UR, Mg ²⁺	Human urine	10–90	0.4	[27]
AuNPs@GO/PPy/CFP ²	DPV	7.0	UA, AA, DA	Human urine RR: 96.8–109%	2–360	1.68	[30]
AuNPs-GO/Au-IDA ³	CV	7.0	UA, AA, DA, G, E	Human urine	2–1050	0.62	[28]
GCE-PErGO-AuNP ⁴	CV, DPV	7.4	UA, AA, DA	Human urine	20–260	20	[31]
AuRGO/GCE ⁵	DPV	7.0	UA, AA, DA	Human serum RR: 97.5–102%	88–53	1.8	[32]
Au@Pd-RGO/GCE ⁶	DPV	7.0	UA, AA, DA	Human urine RR: 97.1–102.5%	0.02–500; 0.1–350	0.005; 0.02	[33]
PEI/[P ₂ W ₁₆ V ₂ -Au/ PDDA-rGO] ₈ ⁷	DPV	7.0	UA, AA, DA, NaCl, KCl, NH ₄ Cl, L-Cys, L-Glu, CA, UR, G	Human urine RR: 95.2–103.1%	0.25–1500	0.08	[34]
rGO-PAMAM-CNT-Au ⁸	DPV	4.0	UA, AA, DA	-	1–114	0.33	[35]

Table 2. Cont.

Electrode	Technique	pH	Interference	Biological Sample. Relative Recovery (RR)	UA Linear Range (μM)	UA LOD (μM)	Ref.
Naf/AuNPs/AzA/MWCNTs ⁹	DPV	7.0	UA, AA, DA, Trp, Na ⁺ , K ⁺ , Ca ²⁺ , Mg ²⁺ , G, citric acid, tartaric acid	Human urine RR: 99.7–103%	0.5–50	0.28	[36]
ITO-rGO-AuNPs ¹⁰	LSV	8.0	UA, AA, Cl, Na ⁺ , Ca ²⁺ NH ₄ ⁺	Human urine, milk	10–500	3.6	[65]
EGFET-AuE ¹¹	-	7.0	UA, AA, G, bilirubin, hemoglobin	Human urine, serum	1–1000	0.5	[16]

AA = ascorbic acid, CA = citric acid, Cys = cysteine, DA = dopamine, E = epinephrine, G = glucose, Glu = glutamate, LSV = linear sweep voltammetry, Trp = tryptophan, UA = uric acid, UR = urea. ¹ = Gold nanorod-decorated graphene oxide glassy carbon electrode; ² = Gold nanoparticles-decorated polypyrrole/graphene oxide nanosheets; ³ = Gold interdigitated microelectrodes array modified with graphene oxide and doped with gold nanoparticles; ⁴ = Gold nanoparticles deposition on reduced graphene oxide based on glassy carbon electrode; ⁵ = Reduced graphene oxide and gold nanoplates-modified glassy carbon electrode; ⁶ = Reduced graphene oxide-supported bimetallic, gold-palladium nanocomposites; ⁷ = Poly(diallyldimethylammonium chloride)-functionalized reduced graphene oxide and polyoxometalates-doped gold nanoparticles sensor; ⁸ = sensor based on reduced graphene oxide functionalized by poly(amido-amine), multi-walled carbon nanotubes and gold nanoparticles; ⁹ = Nafion-based electrode modified with Azure A-coated carbon nanotubes coated with gold nanoparticles; ¹⁰ = polyethylene terephthalate substrate coated with indium tin oxide and combined with reduced graphene oxide and gold nanoparticles; ¹¹ = 11-(ferrocenyl)undecanethiol-modified gold electrode.

3.1.3. Chemically Modified Electrodes

Table 3 presents different variants of chemically modified electrodes (CMEs) [74]. Conductive polymers and chemical doping with heteroatoms were used repeatedly for modifying electrodes in the past ten years [74–76]. Conductive polymers act as enhancing materials, with high conductivity, high selectivity, large surface area and light weight.

Polymers combined with graphene oxide (GO) provide satisfactory conductivity due to the π - π links between the polypyrrole and GO layers. Non-reduced GO provides a sufficient quantity of oxygen functional groups to enhance the electrochemical signal for detection of uric acid and interference molecules (AA and DA) [76].

In order to resist the adsorption of nonspecific biomolecules, electrochemical systems using antifouling sensing interfaces were developed. One conductive polymer, poly(3,4-ethylenedioxythiophene) (PEDOT), appears to have higher conductivity, a faster electrochemical response and to be more stable in comparison with polyaniline (PANI) and polypyrrole (Ppy). This is the consequence of its increased flexibility and high porosity, which permit rapid adsorption of the biomolecules [57]. These designs are recommended for their accuracy and sensitivity in detecting different disease biomarkers in complex biological fluids.

These designs show biocompatibility with tissue, great electrochemical stability and broad applicability in electrochemical characterization of different bioactive compounds, such as uric acid, urea, ammonia, glucose and nitrite [57,74–76]. Moreover, polymer film-modified electrodes are a cheaper variant of electrodes with results that are comparable with those of metal electrodes and biosensors [74–76]. Regarding real samples detection, CMEs showed satisfactory results that were in agreement with other types of sensors [74–76].

- A glassy carbon electrode modified with electrochemically reduced graphene oxide (ErGO) and poly(3,4-ethylenedioxythiophene):poly(styrenesulfonate) (PEDOT:PSS).

A recent original article presents a new type of non-enzymatic sensor based on a glassy carbon electrode modified with reduced graphene oxide and a conductive polymer (PEDOT:PSS) [76]. The sensing advantages of utilizing the combination of graphene oxide and conductive polymers have been investigated previously with encouraging results [76–82]. Additionally, it was proven that Poly(3,4-ethylenedioxythiophene):poly(styrenesulfonate), or PEDOT:PSS, improves the conductivity and the stability of the sensor, provides a large electrochemical window and is easily attached to graphene oxide [76–86].

For the configuration of the sensor, the graphene oxide was reduced to ErGO, combined with PEDOT:PSS and doped on a GCE [76]. This sensor was developed for detection of uric acid from standard solutions, but also from artificial saliva, simultaneously with dopamine. The optimal parameters were obtained using CV and DPV techniques by performing the measurements on artificial saliva solution. It was found that the uric acid peak potential was stronger and more stable, according to the DPV measurements, allowing measurement of uric acid at a large range of concentrations from 10 μM to 100 μM . The limit of detection of uric acid was 1.08 μM , which is under the normal human saliva concentration of uric acid. The interference tests successfully exhibited the separation of uric acid and dopamine peaks at 140 mV and 40 mV using standard solutions. Moreover, the sensor displayed reproducibility in detection of uric acid from artificial saliva and also high selectivity when testing for uric acid in human saliva [76].

- Poly(2-(N-morpholine)ethane sulfonic acid)/RGO-modified electrode.

Another conductive polymer-modified electrode has been developed by Zhang et al., for electrochemical identification of uric acid and interferent compounds, the Poly(2-(N-morpholine)ethane sulfonic acid)/RGO electrode [75]. The PMES/RGO/GCE was studied using scanning electron microscopy (SEM) and electrochemical impedance spectroscopy (EIS). The electrochemical detection was performed with both cyclic voltammetry and differential pulse voltammetry techniques, and the optimal pH was found to be 7.0. The uric acid oxidation peak potential was identified with DPV scanning at around 180 mV to 320 mV [75].

The simultaneous detection of AA, DA and UA was successful, with very good separation of the oxidation peaks. The linear ranges for AA, DA and UA were determined as 1.0 mM to 30 mM (30 mM to 100 mM), 0.05 mM to 100 mM, and 0.1 mM to 100 mM, respectively. In addition, the limit of detection for each compound was 0.43 mM, 0.0062 mM and 0.056 mM, respectively. In an interferent study, the electrochemical influences of L-cystine, L-lysine, L-tyrosine, and glucose on a mixture of AA, DA and UA were investigated. The results showed insignificant interference. Finally, the electrode demonstrated good selectivity and stability in testing real samples (human serum) [75].

- Zeolite Imidazolate Framework-11 modified electrode.

Researchers have developed a metalorganic framework (MOF) consisting of a structure with Zn ions and four nitrogen atoms of 4-benzimidazole and named the Zeolite Imidazolate Framework (ZIF-11) [14,52]. This structure has not only great thermal and chemical stability but also an adjustable pore size. ZIF-11 is rarely used for detection of uric acid from urine. The electrode was observed through X-ray diffraction (XRD), scanning electron microscopy (SEM), and nitrogen adsorption/desorption isotherms [14].

The study of the electrochemical behavior of uric acid was performed with a differential pulse-anodic stripping voltammetry (DP-ASV) technique in a buffer solution of pH 7. The best linear concentration ranges of uric acid were 20 μM to 540 μM , and the limit of detection was identified at 0.48 μM . Concerning the interference measurements, the ZIF-11/GCE electrode showed high selectivity in the presence of glucose, ascorbic acid, sodium benzoate, saccharine, xanthine, hypoxanthine, KCl, Na_2CO_3 , Na_2SO_4 and CaCO_3 . Furthermore, when testing urine samples, the ZIF-11/GCE electrode exhibited a good recovery of uric acid, from 94.52% to 104.48%, which recommends this method for medical applications [14].

- Screen-printed carbon electrode equipped with vertically-ordered mesoporous silica-nanochannel film.

A new type of screen-printed carbon electrode was constructed using an amino group-modified vertically-ordered mesoporous silica-nanochannel film (VMSF) and electrochemically reduced graphene oxide (ErGO). This configuration showed a sensitive response with a low limit of detection (LOD: 129 nM) in a uric acid concentration range of 0.5 μM to 180 μM [86].

This sensor configuration consists of a conductive adhesion layer (ErGO) that enhances the electrochemical potential and offers good sensitivity. Vertically-ordered mesoporous silica-nanochannel film (VMSF) offers stability, sensitivity and enhanced specificity. This is due to the vertical arrangement of nanochannels and the large number of hydroxyl groups, which offer direct contact with the substrate and improved permeability properties. Additionally, the ultrasmall volume and the large surface of the nanochannels enable higher selectivity by removing undesirable larger molecules and permitting complex electrochemical detection without sample pre-treatment. Moreover, the modification of VMSF with amino groups leads to a shift to positive electrical charge, resulting in better stability in interactions with negatively charged molecules [81,82,86].

To demonstrate the selectivity capacity of the sensor, standard sample measurements were performed in the presence of interferent molecules (ascorbic acid, dopamine, ions- Na^+ , K^+ , Ca^{2+} , Mg^{2+} , glucose and urea). The results showed clear separation of peaks from AA and UA and no interaction with the positively charged molecules [86]. Consequently, this sensor configuration demonstrated enhanced bioactive performance for uric acid detection from whole blood [81,86].

Table 3. Comparison of different CMEs for detection of uric acid.

Electrode	Technique	pH	Interference	Biological Sample; Relative Recovery (RR)	UA Linear Range (μM)	UA LOD (μM)	Ref.
ZIF-11/GCE ¹	DP-ASV	7.0	UA, AA, G, sodium benzoate, saccharine, XA, hypoxanthine, KCl, Na_2CO_3 , Na_2SO_4 , CaCO_3	Human urine RR: 94.5–104.4%	50–540	0.48	[14]
NgB/CPE ²	CV, DPV	7.0	UA, AA, DA	Human urine RR: 99.4–100.4%	12.5–750	5	[74]
ErGO/PEDOT:PSS/GCE ³	DPV	-	UA, DA	Human urine RR: 96.8–109%	10–100	1.08	[76]
PMES/RGO/GCE ⁴	CV	7.0	UA, AA, DA, L-Cys, L-Lys, L-Tyr, G	Human urine RR: 103.35%	0.1–100	0.056	[75]
NG/GCE ⁵	DPV	6.0	UA, AA, DA	-	0.1–20	0.045	[87]
MC/GCE ⁶	CV, DPV	1.0	UA, AA, DA	Synthetic urine RR: 101%	10–150	1.7	[88]
BDG-based electrode ⁷	SWV	2.25	UA	Human urine RR: 95% RR: 95.2–103.1%	8–1000	7.7	[89]
PMB-ERGO/GCE ⁸	SWV	3.0	UA, XA	Human urine RR: 97.8%	0.08–400	0.03	[15]
PEDOT-nf/PGE and Ox-PEDOT-nf/PGE ⁹	CV	2.0	UA	Human urine, serum RR: 104–107%	0.1–20	0.0013	[90]
MWNTs/MGF/GCE ¹⁰	DPV	7.3	UA, AA, DA, Trp, Na^+ , K^+ , Ca^{2+} , Mg^{2+} , G	-	5–100; 300–10,000	0.93	[10]
GCE/tosyl-CNPSE ¹¹	CV	2.0	UA, AA	Human urine RR: 106%	0.1–100	0.2	[91]
CTAB/GO/MWNTs/GCE ¹²	DPV	7.0	UA, AA, DA, NO_2^-	Human urine RR: 99–115%	3–600	1	[92]
EGNWsE ¹³	DPV	7.4	UA, AA, DA	-	2.6–200	0.000033	[93]
GEF/CFE ¹⁴	DPV	7.0	UA, AA, DA	Human urine, serum	3.98–371	2	[94]
Trp-GR/GCE ¹⁵	DPV	7.0	UA, AA, DA	Human urine RR: 97.3–99.9% Human serum RR: 92.6–98.7%	10–1000	1.24	[95]

Table 3. Cont.

Electrode	Technique	pH	Interference	Biological Sample; Relative Recovery (RR)	UA Linear Range (μM)	UA LOD (μM)	Ref.
NH ₂ -VMSF/ErGO/SPCE ¹⁶	DPV	5.0	UA, AA, DA, G, UR, Na ⁺ , K ⁺ , Ca ²⁺ , Mg ²⁺	Human whole blood RR: 99.0–107.0%	0.5–180	0.129	[86]

AA = ascorbic acid, DA = dopamine, G = glucose, L-Cys = L-cystine, L-Lys = L-lysine, L-Tyr = L-tyrosine, SWV = square wave voltammetry, Trp = tryptophan, UA = uric acid, UR = urea, XA = xanthine; ¹ = Zeolite Imidazolate Framework-11-modified electrode; ² = Poly (Naphthol Green B)-film-modified carbon paste electrode; ³ = Gold nanoparticle-decorated polypyrrole/graphene oxide nanosheets; ⁴ = Poly(2-(N-morpholine)ethane sulfonic acid)/RGO-modified electrode; ⁵ = Nitrogen-doped graphene; ⁶ = Microporous carbon electrode; ⁷ = Boron-doped diamond electrode; ⁸ = Poly(Methylene Blue) and electrochemically reduced graphene oxide composite film-modified electrode; ⁹ = Over-oxidized poly(3,4-ethylenedioxythiophene) nanofiber-modified pencil graphite electrode; ¹⁰ = A multi-walled carbon nanotubes (MWNTs) bridged mesocellular graphene foam (MGF) nanocomposite (MWNTs/MGF)-modified glassy carbon electrode; ¹¹ = Tosyl surface carbon nanoparticles/glassy carbon electrode; ¹² = Hexadecyl trimethyl ammonium bromide (CTAB)-functionalized graphene oxide (GO)/multi-walled carbon nanotubes (MWNTs)-modified glassy carbon electrode; ¹³ = Three-dimensional (3D) unmodified 'as-grown' epitaxial graphene nanowall arrays (EGNWs); ¹⁴ = Carbon fiber electrode (CFE) modified by graphene flowers; ¹⁵ = Tryptophan-functionalized graphene nanocomposite (Trp-GR); ¹⁶ = Screen-printed carbon electrode equipped with vertically-ordered mesoporous silica-nanochannel film.

3.2. Biosensors for Detection of Uric Acid

Biosensor electrodes demonstrate good sensitivity over time but have greater cost and stability issues [23]. There are three processes involved in biosensing: measuring the concentration of an active redox substrate or product (e.g., H₂O₂); detection of resulting potential from electron exchange in the enzyme-transducer site; or direct electron transfer at the exchange site between the enzyme and electrode surface [23].

In the uric acid domain, studies encompass many interventions related to the surface of electrodes for improving the biosensing capacity and integrating uricase [23]. Most studies report different modifications with conductive polymers [23,96–100], transition metal oxides nanocomposites [55,101–103], and different configurations of low-dimensional carbon nanomaterials [69–74].

In addition to these, some new biosensors have proven their effectiveness for determining uric acid from different standard mixtures and from real samples. Table 4 presents a comparison of the latest biosensors developed for detection of uric acid. Most of the biosensors compared have proven high sensitivity, with LOD values from 0.15 μM to 0.83 μM [23,96–98,103] and also good selectivity in real samples [23,96–98,103,104]. The most sensitive of these electrodes are outlined below [96–98,100,102,103].

- Zinc tetraaminophthalocyanine-functionalized graphene nanosheets/GCE with uricase.

Phthalocyanine (Pc) is an organic molecule which demonstrates stable biochemical interactions with transition metal ions, forming metallophthalocyanines (MPcs), and also with reduced graphite oxide [103]. π - π non-covalent interactions can be established between MPcs and rGO for better electrochemical potency. Moreover, MPcs has prosthetic groups of heme enzymes, making it conducive to faster electron transfer, in particular by modification with uricase. Therefore, the new biosensor zinc tetraaminophthalocyanine-functionalized graphene nanosheets/GCE with uricase show a high electrochemical capacity for detection of uric acid. This was confirmed by testing for uric acid under optimized conditions. The concentration range optimized for detection of uric acid was between 0.5 μM and 100 μM , and the detection limit was very low at 0.15 μM . This biosensor exhibits reasonable sensitivity in human urine samples, which suggests it as one of the best devices for the detection of uric acid [103].

- The ferrocene-conjugated uricase biosensor on a nafion polymer membrane.

The ferrocene-conjugated uricase biosensor comprises a nafion polymer membrane deposited on a glassy carbon electrode, which enhances the enzyme stability and catalytic efficiency of the biosensor [23]. The structure and morphology of the biosensor was studied

by AFM, ATR-FTIR and EDX. The optimization of uric acid detection was performed with differential pulse voltammetry (DPV) and amperometry in a 7.4 phosphate buffer solution. Measurements showed the uric acid oxidation peak at 0.370 V and two concentrations ranges: 500 nM to 50 μ M, and 25 μ M to 600 μ M. The lower limit of detection was registered at 0.23 μ M. The biosensor showed a good reproducibility response (coefficients of variation: 1.6% and 2.1%) and also very good selectivity in terms of interference in serum samples (confidence limit: >95%) [23].

- Uricase-thionine-single-walled carbon nanotube-modified electrode

The uricase-thionine-single-walled carbon nanotube-modified electrode functions by detecting H_2O_2 that results from the enzymatic redox process [96]. The biosensor is composed of an enzyme (uricase) deposited on a low-dimensional carbon nanomaterial (SWNTs) and enhanced with a positively charged dye molecule (Th). The formed nanostructure works as a mediator to the uricase and performs accurate uric acid detection. The limit of detection was noted at 0.05 μ M, with a large concentration window of 2 μ M to 2000 μ M. Furthermore, the biosensor showed good stability and reproducibility. An interference study was performed in the presence of ascorbic acid, 3,4-dihydroxyphenylacetic acid, 4-acetamidophenol and other compounds with a standard solution and also on real samples. In terms of applicability, UOx-Th-SWNTs/GC exhibited good selectivity with cell lysate and serum samples [96].

Table 4. Comparison of biosensors for detection of uric acid.

Electrode	Technique	pH	Interference	Biological Sample. Relative Recovery (RR)	UA Linear Range (μ M)	UA LOD (μ M)	Ref.
UOx/CNT/CMC ¹	CV	7.4	UA, AA, UR	Human urine, serum RR: 96.3%	20–5000	2.8	[101]
RGO/AuNP hybrid film ²	Amperometry	7.6	UA, AA, DA	-	-	1	[55]
UOx-Th-SWNTs/GC ³	-	-	UA, AA, 3,4-dihydroxyphenylacetic acid, 4-acetamidophenol	HEK 293A cells RR: 100.9–101.4%	2–2000	0.5	[96]
UOx/PBG/CNT/CFE and UOx PTH/CNT/CFE ⁴	Amperometry	7.0	UA, AA, G, citric acid, creatinine, NH_4^+ , phenol, UR	Human urine RR: 95–105%	2–100	0.6	[97]
UOx/rGO/ZnPc-NH ₂ /GCE ⁵	-	-	UA	Human urine RR: 92.5–97.6%	0.5–100	0.15	[103]
MP/SWCNT/SPE ⁶	CV	7.4	UA, AA, DA	Human urine	0.001–0.20	0.83	[98]
UOx/AuNP/c-MWCNT/Au ⁷	CV	7.5	UA, AA, G, chol, UR, pyruvate, bilirubin, $CuSO_4$, KCl, FAD, NaCl, $ZnSO_4$, NADH, $CaCl_2$, EDTA, NEM, riboflavin, $MnCl_2$, FM	Human serum RR: 95–97%	5–800	5	[102]
UOx-PANI-PB-PtE ⁸	CV	7.2	UA, AA, UR, G	Human serum	10–160	2.6	[99]
UOx-PANI-MWCNT/ITO ⁹	CV, DPV	-	UA	Human serum	10–1000	10	[100]
UOx/Nafion/ZnO-NFs/Au ¹⁰	Amperometry	7.4	UA, AA, UR, G	-	0.5–1500	0.5	[104]
Naf/UOx/Fc/GCE ¹¹	DPV, Amperometry	7.4	UA, AA, DA, UR, G, XA	Human serum RR: 95%	0.5–50; 25–600	0.23	[23]

AA = ascorbic acid, Chol = cholesterol, DA = dopamine, G = glucose, UA = uric acid, UR = urea. ¹ = Uricase/carbon nanotube/carboxymethylcellulose electrode; ² = Large-scale graphene film doped with gold nanoparticles; ³ = uricase – thionine – single-walled carbon nanotube-modified electrodes; ⁴ = Poly(brilliant green) and poly(thionine)-modified carbon nanotube-coated carbon film electrode; ⁵ = Zinc tetraaminophthalocyanine-functionalized graphene nanosheets/GCE with uricase; ⁶ = Magnetically entrapped SWCNT; ⁷ = chitosan–glutaraldehyde crosslinked uricase immobilized onto Prussian blue nanoparticles (PBNPs) absorbed onto carboxylated multi-walled carbon nanotube (c-MWCNT) and polyaniline (PANI) layer, electrochemically deposited on the surface of Au electrode; ⁸ = Uricase-immobilized Polyaniline/Prussian blue (PANI-PB) composite on a platinum electrode (PtE); ⁹ = Uricase immobilized onto multi-walled carbon nanotubes (CNT) doped polyaniline (PANI) nanocomposite-indium tin oxide (ITO)-coated glass substrate; ¹⁰ = Uricase immobilized in conjunction with Nafion onto zinc oxide nanoflakes (ZnO-NF) and a gold-coated glass substrate; ¹¹ = Ferrocene (Fc)-induced electro-activated uricase (UOx) deposited within Nafion (Naf) on glassy carbon electrode (GCE).

4. Challenges and Perspectives of Uric Acid Electrochemical Detection

Among the transition metal oxide-modified electrodes, ZnO NWAs/GF/GCE [24] had the best performance in terms of sensitivity, but highly selective sensors with moderately higher limits of detection included GCE/MC-GO-Fe₃O₄ [37], CuO/GCE [40] and RuON-GCE [51] (Table 1).

From Table 2, it can be noted that some gold-coated sensors demonstrated very good anti-interference response in real samples, including Au@Pd-RGO [33], PEI/[P2W16V2-Au/PDDA-rGO]⁸ [34], GO/AuNR/GCE [27], ITO-rGO-AuNPs [66], GCE-PErGO-AuNP [31], and Nafion/AuNPs/AzA/MWCNTs [36]. The Au@Pd-RGO [33] sensor had the lowest limit of detection of 0.005 μ M [33] for isolated detection of uric acid.

Regarding the chemosensors, most of the sensors are highly sensitive for detection of uric acid (Table 3). Some sensors demonstrated good sensitivity and higher specificity, including ZIF-11/GCE [14], boron-doped diamond electrode [92], over-oxidized poly(3,4-ethylenedioxythiophene) nanofibers/PGE [90], and tosyl surface carbon nanoparticles/GCE [91]. Table 4 shows a large variety of biosensors with good and high selectivity for uric acid from real samples: zinc tetraaminophthalocyanine-functionalized graphene nanosheets/GCE with uricase [103], poly(brilliant green) and poly(thionine)-modified carbon nanotube-coated carbon film electrode [97], magnetically entrapped SWCNT [98], uricase/carbon nanotube/carboxymethylcellulose electrode [101], UOx/AuNP/c-MWCNT/Au [102], and Naf/UOx/Fc/GCE [19]. The most sensitive biosensor among those analyzed was the zinc tetraaminophthalocyanine-functionalized graphene nanosheets/GCE with uricase [103] with a limit of detection of 0.15 μ M [103].

Considering future medical technologies, nanoparticles (NPs) will be central to developing new sensing devices because of their extremely small dimensions in the nanometer (nm) range, wide availability (found in nature or laboratory manufactured) and electrochemical properties [105,106].

The outlook for uric acid electroanalysis involves different configurations of nanocomposites. Carbon nanotubes (CNTs), including multi-walled nanotubes (MWCNTs) and single-walled nanotubes (SWCNTs) [107], are the most preferred for wide range of biological metabolites [108–111] because of their large specific surface area, enhanced activity and great stability. Moreover, nanocomposites amplify the electron transfer, resulting in a rapid and higher potential response [107].

The latest research is investigating sensors based on carbon nanotubes modified with lanthanum hydroxide (La(OH)₃) [112], Zn_MM [113], cobalt phthalocyanine [107] or bentonite (Bent) and L-cysteine [114].

The scientific literature [115] also mentions different approaches and emerging strategies to develop reliable biosensors that consider different active and passive anti-biofouling strategies (Figure 3), thereby extending their applications to biological samples for clinical diagnostics, personalized medicine, point-of-care testing, and wearable devices.

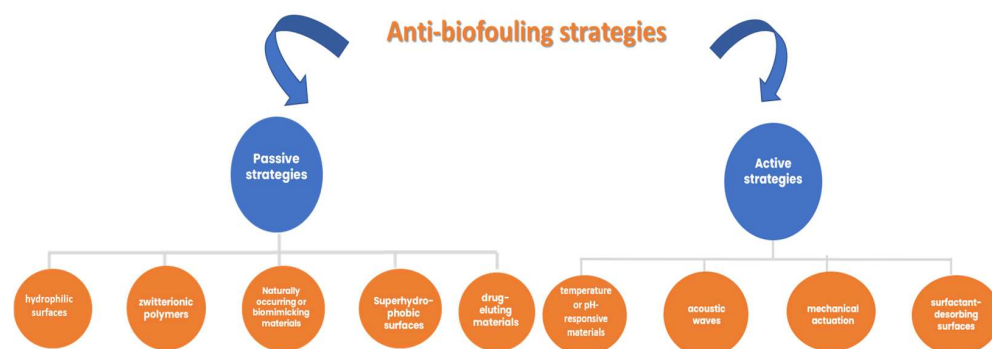


Figure 3. Anti-biofouling strategies.

The abovementioned anti-biofouling strategies aim to delay the biofouling process and remove the accumulation of different bioactive compounds, if necessary. There is

also the possibility of using combinations of different materials (materials with natural morphology and surface stability) and transducers to achieve a better long-term reliability.

5. Conclusions

This review collates findings concerning recently developed sensing devices for the detection of uric acid in the presence of interferent compounds, investigating their possible use as point-of-care technologies. In the research field of uric acid electroanalysis, the developed sensors demonstrated high sensitivity, very good specificity and rapid response in biological fluids, such as whole blood, human serum, urine, and saliva. In comparison with conventional tests for urinalysis, such as spectroscopy, chromatography, membrane capillary electrophoresis, and spectrophotometric methods, sensors proved to be better suited from the point of view of rapid quantification, reusability and costs. Additionally, in comparison with the dipstick test, sensors are more sensitive and specific, providing much more exact quantification of the substrate analyzed [105].

Reviewing the past ten years of developments in uric acid sensors, it can be observed that there is an increasing trend towards using polymeric nanostructures to enhance the electrode's catalytic activity [116]. In addition, low-dimensional carbon nanomaterials are still preferred for their exceptional performance in electrical conductivity and the formation of strong bonds with positive charge materials [116]. Biosensors are also undergoing constant development and improvement, ensuring remarkable results in the detection of uric acid.

Among the articles reviewed, the best results regarding the limit of detection and concentration range were reported for the 3D unmodified 'as-grown' epitaxial graphene nanowall arrays (EGNWs), which were distinguished by an extremely and unprecedented low limit of detection of 0.033 nM (Table 4) [93].

Overall, the majority of the described sensors had satisfactory results in relation to the electrochemical activity of uric acid. In particular, a higher catalytic performance was identified at chemically modified electrodes (Table 3). The anti-interference capacity was studied in all cases using standard solutions and also real samples (human urine, serum, milk, saliva), but the best results were obtained by biosensors (Table 4).

Accordingly, a large variety of sensors and biosensors are suitable for medical applications, such as screening for hyperuricemia or gout, or as adjuvant in the diagnosis of other medical conditions.

Author Contributions: Conceptualization, L.C. and M.B.; writing—original draft preparation, L.C.; writing—review and editing, L.C., M.B. and L.E.G.; visualization, all authors; supervision, M.B. All authors have read and agreed to the published version of the manuscript.

Funding: This research received no external funding.

Conflicts of Interest: The authors declare no conflict of interest.

References

1. Islam, M.N.; Ahmed, I.; Anik, M.I.; Ferdous, M.S.; Khan, M.S. Developing Paper Based Diagnostic Technique to Detect Uric Acid in Urine. *Front. Chem.* **2018**, *6*, 496. [[CrossRef](#)]
2. Benn, C.L.; Dua, P.; Gurrell, R.; Loudon, P.; Pike, A.; Storer, R.I.; Vangjeli, C. Physiology of Hyperuricemia and Urate-Lowering Treatments. *Front. Med.* **2018**, *5*, 160. [[CrossRef](#)]
3. Chong, D.P. Theoretical Study of Uric Acid and its Ions in Aqueous Solution. *J. Theor. Comput. Sci.* **2013**, *1*. [[CrossRef](#)]
4. Desideri, G.; Castaldo, G.; Lombardi, A.; Mussap, M.; Testa, A.; Pontremoli, R.; Punzi, L.; Borghi, C. Is it time to revise the normal range of serum uric acid levels? *Eur. Rev. Med. Pharmacol. Sci.* **2014**, *18*, 1295–1306.
5. de Lassichere, C.; Latapie, L.; Evrard, D.; Gros, P. New Insight into the EC' Mechanism of Uric Acid Regeneration in the Presence of Ascorbic Acid on a Poly(3,4-ethylenedioxythiophene) Modified Gold Electrode. *Electroanalysis* **2018**, *30*, 1653. [[CrossRef](#)]
6. Sajid, M.; Nazal, K.M.; Mansha, M.; Alsharaa, A.; Jillani, S.M.S.; Basheer, C. Chemically modified electrodes for electrochemical detection of dopamine in the presence of uric acid and ascorbic acid: A review. *Trends Anal. Chem.* **2016**, *76*, 15–29. [[CrossRef](#)]
7. Lupu, S.; Lete, C.; Balaure, P.C.; Caval, D.I.; Mihailciuc, C.; Lakard, B.; Hihn, J.Y.; Del Campo, F.J. Development of amperometric biosensors based on nanostructured tyrosinase-conducting polymer, composite Electrodes. *Sensors* **2013**, *13*, 6759–6774. [[CrossRef](#)] [[PubMed](#)]

8. Tan, B.L.; Norhaizan, M.E.; Liew, W.-P.-P.; Sulaiman Rahman, H. Antioxidant and Oxidative Stress: A Mutual Interplay in Age-Related Diseases. *Front. Pharmacol.* **2018**, *9*, 1162. [[CrossRef](#)] [[PubMed](#)]
9. Picillo, M.; Santangelo, G.; Moccia Erro, R.; Amboni, M.; Prestipino, E.; Longo, K.; Vitale, C.; Spina, E.; Orefice, G.; Barone, P.; et al. Serum uric acid is associated with apathy in early, drug naive Parkinson's disease. *J. Neural Transm.* **2015**, *2015*, 371–377. [[CrossRef](#)] [[PubMed](#)]
10. Li, H.; Wang, Y.; Ye, D.; Luo, J.; Su, B.; Zhang, S.; Kong, J. An electrochemical sensor for simultaneous determination of ascorbic acid, dopamine, uric acid and tryptophan based on MWNTs bridged mesocellular graphene foam nanocomposite. *Talanta* **2014**, *127*, 255–261. [[CrossRef](#)]
11. Elhag, S.; Ibutoto, Z.H.; Nur, O.; Willander, M. Incorporating β -Cyclodextrin with ZnO nanorods: A potentiometric strategy for selectivity and detection of dopamine. *Sensors* **2014**, *14*, 1654–1664. [[CrossRef](#)]
12. Kumar, S.; Vicente-Beckett, V. Glassy carbon electrodes modified with multiwalled carbon nanotubes for the determination of ascorbic acid by square-wave voltammetry. *Beilstein J. Nanotechnol.* **2012**, *3*, 388–396. [[CrossRef](#)]
13. Levite, M. Dopamine and T cells: Dopamine receptors and potent effects on T cells, dopamine production in T cells, and abnormalities in the dopaminergic system in T cells in autoimmune, neurological and psychiatric diseases. *Acta Physiol.* **2016**, *216*, 42–89. [[CrossRef](#)]
14. Thanh, T.S.; Qui, P.T.; Thanh Tu, N.T.; Toan, T.T.T.; Hoa, T.T.B.; Son, L.V.T.; Nguyen, D.M.; Tuyen, T.N.; Khieu, D.Q. Electrochemical Determination of Uric Acid in Urine by Using Zeolite Imidazolate Framework-11 Modified Electrode. *J. Nanomater.* **2021**, *2021*, 9914062. [[CrossRef](#)]
15. Liu, G.; Wei, M.; Luo, Y.; Sun, D.; Shao, S. Simultaneous determination of uric acid and xanthine using a poly(methylene blue) and electrochemically reduced graphene oxide composite film modified electrode. *J. Anal. Methods Chem.* **2014**, *2014*, 984314. [[CrossRef](#)]
16. Guan, W.; Duan, X.; Reed, M.A. Highly specific and sensitive non-enzymatic determination of uric acid in serum and urine by extended gate field effect transistor sensors. *Biosens. Bioelectron.* **2014**, *51*, 225–231. [[CrossRef](#)]
17. Tadese, A.; Subramanian, P.A.; Woldu, A.; Pal, R. Electrochemical determination and comparison of ascorbic acid in freshly prepared and bottled fruit juices: A cyclic voltammetric study. *J. Chem. Pharm. Res.* **2014**, *6*, 880–888.
18. Carr, A.C.; Shaw, G.M.; Fowler, A.A.; Natarajan, R. Ascorbate-dependent vasopressor synthesis: A rationale for vitamin C administration in severe sepsis and septic shock? *Crit. Care* **2015**, *19*, 418. [[CrossRef](#)]
19. Ide, K.; Yamada, H.; Umegaki, K.; Mizuno, K.; Kawakami, N.; Hagiwara, Y.; Matsumoto, M.; Yoshida, H.; Kim, K.; Shiosaki, E.; et al. Lymphocyte vitamin C levels as potential biomarker for progression of Parkinson's disease. *Nutrition* **2015**, *31*, 406–408. [[CrossRef](#)] [[PubMed](#)]
20. Jiang, Y.; Wang, B.; Meng, F.; Cheng, Y.; Zhu, C. Microwave-assisted preparation of N-doped carbon dots as a biosensor for electrochemical dopamine detection. *J. Colloid Interface Sci.* **2015**, *452*, 199–202. [[CrossRef](#)] [[PubMed](#)]
21. Chairam, S.; Sriraska, W.; Amatongchai, M.; Somsook, E. Electrocatalytic oxidation of ascorbic acid using a poly (aniline-co-m-ferrocenylaniline) modified glassy Carbon Electrode. *Sensors* **2014**, *11*, 10166–10179. [[CrossRef](#)]
22. Fernandes, D.M.; Costa, M.; Pereira, C.; Bachiller-Baeza, B.; Rodriguez-Ramos, I.; Guerrero-Ruiz, A.; Freire, C. Novel electrochemical sensor based on N-doped carbon nanotubes and Fe₃O₄ nanoparticles: Simultaneous voltammetric determination of ascorbic acid, dopamine and uric acid. *J. Colloid Interface Sci.* **2014**, *432*, 207–213. [[CrossRef](#)]
23. Ghoh, T.; Sarkar, P.; Turner, A.P.F. A novel third generation uric acid biosensor using uricase, electro-activated with ferrocene on a Nafion coated glassy carbon electrode. *Bioelectrochemistry* **2015**, *102*, 1–9. [[CrossRef](#)]
24. Yue, H.Y.; Huang, S.; Chang, J.; Heo, C.; Yao, F.; Adhikari, S.; Gunes, F.; Liu, L.C.; Lee, T.H.; Oh, E.S.; et al. ZnO Nanowire arrays on 3D hierarchical graphene foam: Biomarker detection of Parkinson's disease. *ACS Chem. Neurosci.* **2014**, *8*, 1639–1646. [[CrossRef](#)]
25. Wu, Y.; Deng, P.; Tian, Y.; Feng, J.; Xiao, J.; Li, J.; Liu, J.; Li, G.; He, Q. Simultaneous and sensitive determination of ascorbic acid, dopamine and uric acid via an electrochemical sensor based on PVP-graphene composite. *J. Nanobiotechnol.* **2020**, *18*, 112. [[CrossRef](#)]
26. Vrabelj, T.; Finšgar, M. Recent Progress in Non-Enzymatic Electroanalytical Detection of Pesticides Based on the Use of Functional Nanomaterials as Electrode Modifiers. *Biosensors* **2022**, *12*, 263. [[CrossRef](#)] [[PubMed](#)]
27. Safitri, H.; Wahyuni, W.T.; Rohaeti, E.; Khalil, M.; Marken, F. Optimization of uric acid detection with Au nanorod-decorated graphene oxide (GO/AuNR) using response surface methodology. *RSC Adv.* **2022**, *12*, 25269–25278. [[CrossRef](#)] [[PubMed](#)]
28. Abellán-Llobregat, A.; Vidal, L.; Rodríguez-Amaro, R.; Berenguer-Murcia, A.; Canals, A.; Morallón, E. Au-IDA Microelectrodes Modified with Au-Doped Graphene Oxide for the Simultaneous Determination of Uric Acid and Ascorbic Acid in Urine Samples. *Electrochim. Acta* **2017**, *227*, 275–284. [[CrossRef](#)]
29. Schlesinger, O.; Lital, A. Encapsulation of Microorganisms, Enzymes, and Redox Mediators in Graphene Oxide and Reduced Graphene Oxide. *Methods Enzymol.* **2018**, *609*, 197–219. [[PubMed](#)]
30. Tan, C.; Zhao, J.; Sun, P.; Zheng, W.; Cui, G. Gold Nanoparticle Decorated Polypyrrole/Graphene Oxide Nanosheets as a Modified Electrode for Simultaneous Determination of Ascorbic Acid, Dopamine and Uric Acid. *New. J. Chem.* **2020**, *12*, 4916–4926. [[CrossRef](#)]
31. Imran, H.; Palinci, N.M.; Venkataraman, D. Facile and Green Synthesis of Graphene Oxide by Electrical Exfoliation of Pencil Graphite and Gold Nanoparticle for Non-Enzymatic Simultaneous Sensing of Ascorbic Acid, Dopamine and Uric Acid. *RSC Adv.* **2015**, *78*, 63513–63520. [[CrossRef](#)]

32. Wang, C.; Du, J.; Wang, H.; Zou, C.; Jiang, F.; Yang, P.; Du, Y. A Facile Electrochemical Sensor Based on Reduced Graphene Oxide and Au Nanoplates Modified Glassy Carbon Electrode for Simultaneous Detection of Ascorbic Acid, Dopamine and Uric Acid. *Sens. Actuators B Chem.* **2014**, *204*, 302–309. [[CrossRef](#)]
33. Jiang, J.; Du, X. Sensitive Electrochemical Sensors for Simultaneous Determination of Ascorbic Acid, Dopamine, and Uric Acid Based on Au@Pd-Reduced Graphene Oxide Nanocomposites. *Nanoscale* **2014**, *19*, 11303–11309. [[CrossRef](#)]
34. Bai, Z.; Zhou, C.; Xu, H.; Wang, G.; Pang, H.; Ma, H. Polyoxometalates-Doped Au Nanoparticles and Reduced Graphene Oxide: A New Material for the Detection of Uric Acid in Urine. *Sens. Actuators B Chem.* **2017**, *243*, 361–371. [[CrossRef](#)]
35. Wang, S.; Zhang, W.; Zhong, X.; Chai, Y.; Yuan, R. Simultaneous Determination of Dopamine, Ascorbic Acid and Uric Acid Using a Multi-Walled Carbon Nanotube and Reduced Graphene Oxide Hybrid Functionalized by PAMAM and Au Nanoparticles. *Anal. Methods* **2015**, *4*, 1471–1477. [[CrossRef](#)]
36. Filik, H.; Avan, A.A.; Aydar, S. Simultaneous Detection of Ascorbic Acid, Dopamine, Uric Acid and Tryptophan with Azure A-Interlinked Multi-Walled Carbon Nanotube/Gold Nanoparticles Composite Modified Electrode. *Arab. J. Chem.* **2016**, *3*, 471–480. [[CrossRef](#)]
37. Sohoul, E.; Khosrowshahi, E.M.; Radi, P.; Naghian, E.; Rahimi-Nasrabadi, M.; Ahmadi, F. Electrochemical sensor based on modified methylcellulose by graphene oxide and Fe₃O₄ nanoparticles: Application in the analysis of uric acid content in urine. *J. Electroanal. Chem.* **2020**, *877*, 114503. [[CrossRef](#)]
38. Liao, C.; Li, Y.; Tjong, S.C. Graphene Nanomaterials: Synthesis, Biocompatibility, and Cytotoxicity. *Int. J. Mol. Sci.* **2018**, *19*, 3564. [[CrossRef](#)]
39. Rajeswari, B.; Reddy, K.V.N.S.; Devi, A.S.; Madhavi, G.; Reddy, I.R.V.S. Determination of Uric Acid Using TiO₂ Nanoparticles Modified Glassy Carbon Electrode. *Biointerface Res. Appl. Chem.* **2022**, *12*, 6058–6065.
40. Buledi, J.; Ameen, S.; Memon, S.; Fatima, A.; Solangi, A.; Mallah, A.; Karimi, F.; Malakmohammadi, S.; Agarwal, S.; Gupta, V. An Improved Non-Enzymatic Electrochemical Sensor Amplified with CuO Nanostructures for Sensitive Determination of Uric Acid. *Open. Chem.* **2021**, *19*, 481–491. [[CrossRef](#)]
41. Dubey, R.S.; Krishnamurthy, K.V.; Singh, S. Experimental Studies of TiO₂ Nanoparticles Synthesized by Sol-Gel and Solvothermal Routes for DSSCs Application. *Results Phys.* **2019**, *14*, 102390. [[CrossRef](#)]
42. Wei, Y.; Liu, Y.; Xu, Z.; Wang, S.; Chen, B.; Zhang, D.; Fang, Y. Simultaneous Detection of Ascorbic Acid, Dopamine, and Uric Acid Using a Novel Electrochemical Sensor Based on Palladium Nanoparticles/Reduced Graphene Oxide Nanocomposite. *Int. J. Anal. Chem.* **2020**, *2020*, 8812443. [[CrossRef](#)] [[PubMed](#)]
43. Manna, S.; Kumar, S.; Sharma, A.; Sahoo, S.; Dey, M.K.; Mishra, P.K.; Satpati, A.K. rGO/ReO₃ nano composite modified electrode for the ultra-sensitive determination of dopamine and uric acid. *Biosens. Bioelectron. X* **2022**, *11*, 100156. [[CrossRef](#)]
44. Yin, F.Z.; Wu, L.; Yang, H.G.; Su, Y.H. Recent Progress in Biomedical Applications of Titanium Dioxide. *Phys. Chem. Chem. Phys.* **2013**, *14*, 4844. [[CrossRef](#)] [[PubMed](#)]
45. Sousa, S.V.; Corniciuc, C.; Teixeira, M.R. The effect of TiO₂ nanoparticles removal on drinking water quality produced by conventional treatment C/F/S. *Water Res.* **2017**, *109*, 1–12. [[CrossRef](#)] [[PubMed](#)]
46. Mahmoud, W.M.M.; Rastogi, T.; Kümmerer, K. Application of Titanium Dioxide Nanoparticles as a Photocatalyst for the Removal of Micropollutants Such as Pharmaceuticals from Water. *Curr. Opin. Green. Sustain. Chem.* **2017**, *6*, 1–10. [[CrossRef](#)]
47. Shetti, N.P.; Nayak, D.S.; Malode, S.J.; Kulkarni, R.M. Electrochemical Sensor Based upon Ruthenium Doped TiO₂ Nanoparticles for the Determination of Flufenamic Acid. *J. Electrochem. Soc.* **2017**, *164*, 3036–3042. [[CrossRef](#)]
48. Wang, H.-M.; Wang, C.-C.; Wang, A.-J.; Zhang, L.; Luo, X.; Yuan, P.-X.; Feng, J.-J. Green synthesis of Pd nanocones as a novel and effective electrochemiluminescence illuminant for highly sensitive detection of dopamine. *Sens. Actuators B Chem.* **2019**, *281*, 588–594. [[CrossRef](#)]
49. Zhang, Q.; Zhang, K.; Xu, D.; Yang, G.; Huang, H.; Nie, F.; Liu, C.; Yang, S. CuO Nanostructures: Synthesis, Characterization, Growth Mechanisms, Fundamental Properties, and Applications. *Prog. Mater. Sci.* **2014**, *60*, 208–337. [[CrossRef](#)]
50. Sun, D.; Zhao, Q.; Tan, F.; Wang, X.; Gao, J. Simultaneous Detection of Dopamine, Uric Acid, and Ascorbic Acid Using SnO₂ Nanoparticles/Multi-Walled Carbon Nanotubes/Carbon Paste Electrode. *Anal. Methods* **2012**, *10*, 3283. [[CrossRef](#)]
51. Zare, H.R.; Ghanbari, Z.; Nasirizadeh, N.; Benvidi, A. Simultaneous Determination of Adrenaline, Uric Acid, and Cysteine Using Bifunctional Electrocatalyst of Ruthenium Oxide Nanoparticles. *Comptes Rendus Chim.* **2013**, *3*, 287–295. [[CrossRef](#)]
52. Wang, W.Q.; Yue, H.Y.; Yu, Z.M.; Huang, S.; Song, S.S.; Gao, X.; Guan, E.H.; Zhang, H.J.; Wang, Z. Synthesis and Application of MoS₂ Nanosheet Arrays/Carbon Nanofibers for Simultaneous Electrochemical Determination of Levodopa and Uric Acid. *IEEE Sens. J.* **2019**, *15*, 5988–5994. [[CrossRef](#)]
53. Krishnamoorthy, K.; Sudha, V.; Kumar, S.M.S.; Thangamuthu, R. Simultaneous Determination of Dopamine and Uric Acid Using Copper Oxide Nano-Rice Modified Electrode. *J. Alloys Compd.* **2018**, *748*, 338–347. [[CrossRef](#)]
54. Wu, B.; Yeasmin, S.; Liu, Y.; Cheng, L.-Y. Sensitive and selective electrochemical sensor for serotonin detection based on ferrocene-gold nanoparticles decorated multiwall carbon nanotubes. *Sens. Actuators B Chem.* **2022**, *354*, 131216. [[CrossRef](#)]
55. Zhang, P.; Huang, Y.; Lu, X.; Zhang, S.; Li, J.; Wei, G.; Su, Z. One-Step Synthesis of Large-Scale Graphene Film Doped with Gold Nanoparticles at Liquid–Air Interface for Electrochemistry and Raman Detection Applications. *Langmuir.* **2014**, *30*, 8980–8989. [[CrossRef](#)] [[PubMed](#)]

56. Marlinda, A.R.; Sagadevan, S.; Yusoff, N.; Pandikumar, A.; Huang, N.M.; Akbarzadeh, O.; Johan, M.R. Gold Nanorods-Coated Reduced Graphene Oxide as a Modified Electrode for the Electrochemical Sensory Detection of NADH. *J. Alloys Compd.* **2020**, *842*, 156552. [[CrossRef](#)]
57. Tukimin, N.; Abdullah, J.; Sulaiman, Y. Development of a PrGO-Modified Electrode for Uric Acid Determination in the Presence of Ascorbic Acid by an Electrochemical Technique. *Sensors* **2017**, *17*, 1539. [[CrossRef](#)]
58. Akhavan, O.; Bijanzad, K.; Mirsepah, A. Synthesis of Graphene from Natural and Industrial Carbonaceous Wastes. *RSC Adv.* **2014**, *39*, 20441–20448. [[CrossRef](#)]
59. Nikoobakht, B.; El-Sayed, M.A. Preparation and Growth Mechanism of Gold Nanorods (NRs) Using Seed-Mediated Growth Method. *Chem. Mater.* **2003**, *10*, 1957–1962. [[CrossRef](#)]
60. Putra, B.R.; Nisa, U.; Heryanto, R.; Rohaeti, E.; Khalil, M.; Izzataddini, A.; Wahyuni, W.T. A Facile Electrochemical Sensor Based on a Composite of Electrochemically Reduced Graphene Oxide and a PEDOT:PSS Modified Glassy Carbon Electrode for Uric Acid Detection. *Anal. Sci.* **2022**, *1*, 157–166. [[CrossRef](#)]
61. Zhao, Y.; Zhou, J.; Jia, Z.; Huo, D.; Liu, Q.; Zhong, D.; Hu, Y.; Yang, M.; Bian, M.; Hou, C. In-Situ Growth of Gold Nanoparticles on a 3D-Network Consisting of a MoS₂/RGO Nanocomposite for Simultaneous Voltammetric Determination of Ascorbic Acid, Dopamine and Uric Acid. *Microchim. Acta* **2019**, *2*, 92. [[CrossRef](#)] [[PubMed](#)]
62. Hou, J.; Xu, C.; Zhao, D.; Zhou, J. Facile Fabrication of Hierarchical Nanoporous AuAg Alloy and Its Highly Sensitive Detection towards Dopamine and Uric Acid. *Sens. Actuators B Chem.* **2016**, *225*, 241–248. [[CrossRef](#)]
63. Li, W.; Ma, L.; Wu, B.; Zhang, Y.; Li, Z. A Chemically Reduced Graphene Oxide–Au Nanocage Composite for the Electrochemical Detection of Dopamine and Uric Acid. *Anal. Methods* **2017**, *25*, 3819–3824. [[CrossRef](#)]
64. Mahalakshmi, S.; Sridevi, V. In Situ Electrodeposited Gold Nanoparticles on Polyaniline-Modified Electrode Surface for the Detection of Dopamine in Presence of Ascorbic Acid and Uric Acid. *Electrocatalysis* **2021**, *12*, 415–435. [[CrossRef](#)]
65. Mazzara, F.; Patella, B.; Ganci, F.; O’Riordan, A.; Aiello, G.; Torino, C.; Vilasi, A.; Sunseri, C.; Inguanta, R. Flexible Electrode Based on Gold Nanoparticles and Reduced Graphene Oxide for Uric Acid Detection Using Linear Sweep Voltammetry. *Chem. Eng. Trans.* **2021**, *87*, 421–426.
66. Liu, K.; Zhang, J.; Yang, G.; Wang, C.; Zhu, J.-J. Direct Electrochemistry and Electrocatalysis of Hemoglobin Based on Poly(Diallyldimethylammonium Chloride) Functionalized Graphene Sheets/Room Temperature Ionic Liquid Composite Film. *Electrochem. Commun.* **2010**, *3*, 402–405. [[CrossRef](#)]
67. Xu, Z.; Gao, N.; Dong, S. Preparation and Layer-by-Layer Self-Assembly of Positively Charged Multiwall Carbon Nanotubes. *Talanta* **2006**, *3*, 753–758. [[CrossRef](#)]
68. Shi, X.; Wang, S.; Meshinchi, S.; Van Antwerp, M.E.; Bi, X.; Lee, I.; Baker, J.R., Jr. Dendrimer-Entrapped Gold Nanoparticles as a Platform for Cancer-Cell Targeting and Imaging. *Small* **2007**, *7*, 1245–1252. [[CrossRef](#)]
69. Antoni, P.; Hed, Y.; Nordberg, A.; Nyström, D.; von Holst, H.; Hult, A.; Malkoch, M. Bifunctional Dendrimers: From Robust Synthesis and Accelerated One-Pot Postfunctionalization Strategy to Potential Applications. *Angew. Chem. Int. Ed.* **2009**, *12*, 2126–2130. [[CrossRef](#)]
70. Peng, X.; Pan, Q.; Garry, L.R. Bimetallic Dendrimer-Encapsulated Nanoparticles as Catalysts: A Review of the Research Advances. *Chem. Soc. Rev.* **2008**, *8*, 1619. [[CrossRef](#)]
71. Frasconi, M.; Tortolini, C.; Botrè, F.; Mazzei, F. Multifunctional au nanoparticle dendrimer-based surface plasmon resonance biosensor and its application for improved insulin detection. *Anal. Chem.* **2010**, *82*, 7335–7342. [[CrossRef](#)] [[PubMed](#)]
72. Duraisamy, R.; Kiruthiga, P.M.; Yilma, B.; Berekute, A.K. Adsorption of Azure B dye on Rice husk activated carbon: Equilibrium, Kinetic and Thermodynamic Studies. *Int. J. Water Res.* **2015**, *5*, 18–28.
73. Li, N.; Yuan, R.; Chai, Y.; Chen, S.; An, H.; Li, W. New Antibody Immobilization Strategy Based on Gold Nanoparticles and Azure I/Multi-Walled Carbon Nanotube Composite Membranes for an Amperometric Enzyme Immunosensor. *J. Phys. Chem. C* **2007**, *111*, 8443–8450. [[CrossRef](#)]
74. Chitravathi, S.; Kumara Swamy, B.E.; Mamatha, G.P.; Sherigara, B.S. Electrochemical Behavior of Poly (Naphthol Green B)-Film Modified Carbon Paste Electrode and Its Application for the Determination of Dopamine and Uric Acid. *J. Electroanal. Chem.* **2012**, *667*, 66–75. [[CrossRef](#)]
75. Zhang, K.; Zhang, N.; Zhang, L.; Wang, H.; Shi, H.; Liu, Q. Simultaneous voltammetric detection of dopamine, ascorbic acid and uric acid using a poly(2-(N-morpholine)ethane sulfonic acid)/RGO modified electrode. *RSC Adv.* **2018**, *8*, 5280–5285. [[CrossRef](#)] [[PubMed](#)]
76. Gao, N.; Yu, J.; Tian, Q.; Shi, J.; Zhang, M.; Chen, S.; Zang, L. Application of PEDOT:PSS and Its Composites in Electrochemical and Electronic Chemosensors. *Chemosensors* **2021**, *9*, 79. [[CrossRef](#)]
77. Ma, X.; Luo, M.; Gao, W.; Yuan, J.; An, Q.; Zhang, M.; Hu, Z.; Gao, J.; Wang, J.; Zou, Y.; et al. Achieving 14.11% Efficiency of Ternary Polymer Solar Cells by Simultaneously Optimizing Photon Harvesting and Exciton Distribution. *J. Mater. Chem. A* **2019**, *7*, 7843–7851. [[CrossRef](#)]
78. Anand, V.K.; Bukke, A.; Bhatt, K.; Kumar, S.; Sharma, S.; Goyal, R.; Viridi, G.S. Highly Sensitive and Reusable Cu⁺²/Polyaniline/Reduced Graphene Oxide Nanocomposite Ink-Based Non-Enzymatic Glucose Sensor. *Appl. Phys. A* **2020**, *7*, 500. [[CrossRef](#)]
79. Suvina, V.; Murali Krishna, S.; Nagaraju, D.H.; Melo, J.S.; Geetha Balakrishna, R. Polypyrrole-Reduced Graphene Oxide Nanocomposite Hydrogels: A Promising Electrode Material for the Simultaneous Detection of Multiple Heavy Metal Ions. *Mater. Lett.* **2018**, *232*, 209–212. [[CrossRef](#)]

80. Singh, M.; Sahu, A.; Mahata, S.; Shukla, P.; Rai, A.; Rai, V.K. Efficient Electrocatalytic Oxidation of P-Phenylenediamine Using a Novel PANI/ZnO Anchored Bio-Reduced Graphene Oxide Nanocomposite. *New. J. Chem.* **2019**, *17*, 6500–6506. [[CrossRef](#)]
81. Ma, K.; Yang, L.; Liu, J.; Liu, J. Electrochemical Sensor Nanoarchitectonics for Sensitive Detection of Uric Acid in Human Whole Blood Based on Screen-Printed Carbon Electrode Equipped with Vertically-Ordered Mesoporous Silica-Nanochannel Film. *Nanomaterials* **2022**, *12*, 1157. [[CrossRef](#)] [[PubMed](#)]
82. Li, Z.; He, Y.; Klausen, L.H.; Yan, N.; Liu, J.; Chen, F.; Song, W.; Dong, M.; Zhang, Y. Growing vertical aligned mesoporous silica thin film on nanoporous substrate for enhanced degradation, drug delivery and bioactivity. *Bioact. Mater.* **2021**, *6*, 1452–1463. [[CrossRef](#)] [[PubMed](#)]
83. Saadaoui, M.; Fernández, I.; Luna, G.; Díez, P.; Campuzano, S.; Raouafi, N.; Sánchez, A.; Pingarrón, J.M.; Villalonga, R. Label-free electrochemical genosensor based on mesoporous silica thin film. *Anal. Bioanal. Chem.* **2016**, *408*, 7321–7327. [[CrossRef](#)] [[PubMed](#)]
84. Paul, G.; Verma, S.; Jalil, O.; Thakur, D.; Pandey, C.M.; Kumar, D. PEDOT PSS-grafted graphene oxide-titanium dioxide nanohybrid-based conducting paper for glucose detection. *Polym. Adv. Technol.* **2021**, *32*, 1774–1782. [[CrossRef](#)]
85. Promsuwan, K.; Soleh, A.; Saisahas, K.; Saichanapan, J.; Kanatharana, P.; Thavarungkul, P.; Guo, C.; Li, C.M.; Limbut, W. Discrimination of Dopamine by an Electrode Modified with Negatively Charged Manganese Dioxide Nanoparticles Decorated on a Poly(3,4-Ethylenedioxythiophene)/Reduced Graphene Oxide Composite. *J. Colloid Interface Sci.* **2021**, *597*, 314–324. [[CrossRef](#)]
86. Sayyad, P.W.; Sontakke, K.S.; Farooqui, A.A.; Shirsat, S.M.; Tsai, M.-L.; Shirsat, M.D. A Novel Three-Dimensional Electrochemical Cd(II) Biosensor Based on L-Glutathione Capped Poly(3,4-Ethylenedioxythiophene):Polystyrene Sulfonate/Carboxylated Multiwall CNT Network. *J. Sci. Adv. Mater. Devices* **2022**, *7*, 100504. [[CrossRef](#)]
87. Sheng, Z.-H.; Zheng, X.-Q.; Xu, J.-Y.; Bao, W.-J.; Wang, F.-B.; Xia, X.-H. Electrochemical sensor based on nitrogen doped graphene: Simultaneous determination of ascorbic acid, dopamine and uric acid. *Biosens. Bioelectron.* **2012**, *34*, 125–131. [[CrossRef](#)]
88. Rattanaumpa, T.; Maensiri, S.; Ngamchuea, K. Microporous carbon in the selective electro-oxidation of molecular biomarkers: Uric acid, ascorbic acid, and dopamine. *RSC Adv.* **2022**, *12*, 18709–18721. [[CrossRef](#)]
89. Cinkova, K.; Kianičková, K.; Stanković, D.M.; Vojs, M.; Marton, M.; Švorc, L. The doping level of boron-doped diamond electrodes affects the voltammetric sensing of uric acid. *Anal. Methods* **2018**, *10*, 991–996. [[CrossRef](#)]
90. Ozcan, A.; Ilkbas, S. Preparation of poly(3,4-ethylenedioxythiophene) nanofibers modified pencil graphite electrode and investigation of over-oxidation conditions for the selective and sensitive determination of uric acid in body fluids. *Anal. Chim. Acta* **2015**, *891*, 312–320. [[CrossRef](#)] [[PubMed](#)]
91. Amiri, M.; Imanzadeh, H.; Banaei, A. Carbon nanoparticles with tosyl functional group for distinguishing voltammetric peaks of ascorbic acid and uric acid. *Mater. Sci. Eng.* **2015**, *C47*, 189–195. [[CrossRef](#)]
92. Yang, Y.J.; Li, W. CTAB functionalized graphene oxide/multiwalled carbon nanotube composite modified electrode for the simultaneous determination of ascorbic acid, dopamine, uric acid and nitrite. *Biosens. Bioelectron.* **2014**, *56*, 300–306. [[CrossRef](#)]
93. Roy, P.K.; Ganguly, A.; Yang, W.K.; Wu, C.T.; Hwang, J.S.; Tai, Y.; Chen, K.H.; Chen, L.C.; Chattopadhyay, S. Edge promoted ultrasensitive electrochemical detection of organic bio-molecules on epitaxial graphene nanowalls. *Biosens. Bioelectron.* **2015**, *70*, 137–144.
94. Du, J.; Yue, R.; Ren, F.; Yao, Z.; Jiang, F.; Yang, P.; Du, Y. Novel graphene flowers modified carbon fibers for simultaneous determination of ascorbic acid, dopamine and uric acid. *Biosens. Bioelectron.* **2014**, *53*, 220–224. [[CrossRef](#)] [[PubMed](#)]
95. Lian, Q.; He, Z.; He, Q.; Luo, A.; Yan, K.; Zhang, D.; Lu, X.; Zhou, X. Simultaneous determination of ascorbic acid, dopamine and uric acid based on tryptophan functionalized graphene. *Anal. Chim. Acta* **2014**, *823*, 32–39. [[CrossRef](#)] [[PubMed](#)]
96. Chen, D.; Wang, Q.; Jin, J.; Wu, P.; Wang, H.; Yu, S.; Zhang, H.; Cai, C. Low-potential detection of endogenous and physiological uric acid at uricase – thionine – single-walled carbon nanotube modified electrodes. *Anal. Chem.* **2010**, *82*, 2448–2455. [[CrossRef](#)]
97. Ghica, M.E.; Brett, C.M.A. Poly(brilliant green) and poly(thionine) modified carbon nanotube coated carbon film electrodes for glucose and uric acid biosensors. *Talanta* **2014**, *130*, 198–206. [[CrossRef](#)]
98. Herrastia, Z.; Martíneza, F.; Baldrich, E. Detection of uric acid at reversibly nanostructured thin-film microelectrodes. *Sens. Actuators* **2016**, *B234*, 667–673. [[CrossRef](#)]
99. Thakur, B.; Sawant, S.N. Polyaniline/Prussian-Blue-Based Amperometric Biosensor for Detection of Uric Acid. *ChemPlusChem* **2012**, *2*, 166–174. [[CrossRef](#)]
100. Arora, K.; Choudhary, M.; Malhotra, B.D. Enhancing performance of uricase using multiwalled carbon nanotube doped polyaniline. *Appl. Biochem. Biotechnol.* **2014**, *174*, 1174–1187. [[CrossRef](#)]
101. Fukuda, T.; Muguruma, H.; Iwasa, H.; Tanaka, T.; Hiratsuka, A.; Shimizu, T.; Tsuji, K.; Kishimoto, T. Electrochemical Determination of Uric Acid in Urine and Serum with Uricase/Carbon Nanotube/Carboxymethylcellulose Electrode. *Anal. Biochem.* **2020**, *590*, 113533. [[CrossRef](#)]
102. Rawal, R.; Chawla, S.; Chauhan, N.; Dahiya, T.; Pundir, C.S. Construction of amperometric uric acid biosensor based on uricase immobilized on PBNPs/cMWCNT/PANI/Au composite. *Int. J. Biol. Macromol.* **2012**, *50*, 112–118. [[CrossRef](#)]
103. Shi, Y.-M.; Mei, L.; Zhang, J.-X.; Hu, K.; Zhang, X.; Li, Z.-Z.; Miao, M.-S.; Li, X.-M. Synthesis of Zinc Tetraaminophthalocyanine Functionalized Graphene Nanosheets as an Enhanced Material for Sensitive Electrochemical Determination of Uric Acid. *Electroanalysis* **2020**, *7*, 1507–1515. [[CrossRef](#)]
104. Usman, A.S.M.; Ibupoto, Z.H.; Kashif, M.; Hashim, U.; Willander, M. A potentiometric indirect uric acid sensor based on ZnO nanoflakes and immobilized uricase. *Sensors* **2012**, *12*, 2787–2797.

105. Hwang, C.; Lee, W.J.; Kim, S.D.; Park, S.; Kim, J.H. Recent Advances in Biosensor Technologies for Point-of-Care Urinalysis. *Biosensors* **2022**, *12*, 1020. [[CrossRef](#)] [[PubMed](#)]
106. Irkham, I.; Ibrahim, A.U.; Pwavodi, P.C.; Al-Turjman, F.; Hartati, Y.W. Smart Graphene-Based Electrochemical Nanobiosensor for Clinical Diagnosis: Review. *Sensors* **2023**, *23*, 2240. [[CrossRef](#)] [[PubMed](#)]
107. Balogun, S.A.; Fayemi, O.E. Recent Advances in the Use of CoPc-MWCNTs Nanocomposites as Electrochemical Sensing Materials. *Biosensors* **2022**, *12*, 850. [[CrossRef](#)] [[PubMed](#)]
108. Li, Q.; Wang, Z.; Liang, Q.; Zhou, M.; Xu, S.; Li, Z.; Sun, D. Tetra-substituted cobalt (II) phthalocyanine/multi-walled carbon nanotubes as new efficient catalyst for the selective oxidation of styrene using tert-butyl hydroperoxide. *Fuller. Nanotub. Carbon. Nanostruct.* **2020**, *28*, 799–807. [[CrossRef](#)]
109. Şavk, A.; Özdil, B.; Demirkan, B.; Nas, M.S.; Calimli, M.H.; Alma, M.H.; Asiri, A.M.; Şen, F. Multiwalled carbon nanotube-based nanosensor for ultrasensitive detection of uric acid, dopamine, and ascorbic acid. *Mater. Sci. Eng. C* **2019**, *99*, 248–254. [[CrossRef](#)]
110. Wu, B.; Yeasmin, S.; Liu, Y.; Cheng, L.J. Ferrocene Functionalized Gold Nanoparticles on Carbon Nanotube Electrodes for Portable Dopamine Sensor. In Proceedings of the Electrochemical Society Meeting Abstracts 239, Digital Meeting, 30 May–3 June 2021; Volume 55, p. 1345.
111. Musarraf, H.M.; Asiri, A.M.; Uddin, J.; Marwani, H.M.; Rahman, M.M. Development of a L-cysteine Sensor Based on Thallium Oxide Coupled Multi-walled Carbon Nanotube Nanocomposites with Electrochemical Approach. *Chem. Asian J.* **2022**, *17*, e202101117. [[CrossRef](#)]
112. Knežević, S.; Ognjanović, M.; Stanković, V.; Zlatanova, M.; Nešić, A.; Gavrović-Jankulović, M.; Stanković, D. La(OH)₃ Multi-Walled Carbon Nanotube/Carbon Paste-Based Sensing Approach for the Detection of Uric Acid—A Product of Environmentally Stressed Cells. *Biosensors* **2022**, *12*, 705. [[CrossRef](#)] [[PubMed](#)]
113. Negrea, S.; Andelescu, A.A.; Ilies, B.; Motoc, S.; Cretu, C.; Cseh, L.; Rastei, M.; Donnio, B.; Szerb, E.I.; Manea, F. Design of Nanostructured Hybrid Electrodes Based on a Liquid Crystalline Zn(II) Coordination Complex-Carbon Nanotubes Composition for the Specific Electrochemical Sensing of Uric Acid. *Nanomater.* **2022**, *12*, 4215. [[CrossRef](#)] [[PubMed](#)]
114. Choukairi, M.; Bouchta, D.; Bounab, L.; González-Romero, E.; Achache, M.; Draoui, K.; Chaouket, F.; Raissouni, I.; Gharous, M. A Carbon Paste Electrode Modified by Bentonite and L-Cysteine for Simultaneous Determination of Ascorbic and Uric Acids: Application in Biological Fluids. *ChemistryOpen* **2023**, *12*, e202200201. [[CrossRef](#)] [[PubMed](#)]
115. Xu, J.; Lee, H. Anti-Biofouling Strategies for Long-Term Continuous Use of Implantable Biosensors. *Chemosensors* **2020**, *8*, 66. [[CrossRef](#)]
116. Menon, S.; Sam, S.; Keerthi, K.; Kumar, K.G. Carbon Nanomaterial-Based Sensors: Emerging Trends, Markets, and Concerns. *Carbon. Nanomater.-Based Sens.* **2022**, *2022*, 347–379.

Disclaimer/Publisher's Note: The statements, opinions and data contained in all publications are solely those of the individual author(s) and contributor(s) and not of MDPI and/or the editor(s). MDPI and/or the editor(s) disclaim responsibility for any injury to people or property resulting from any ideas, methods, instructions or products referred to in the content.